

SCIENTIFIC REPORTS



OPEN

Endocrine aryl hydrocarbon receptor signaling is induced by moderate cutaneous exposure to ultraviolet light

Babak Memari¹, Loan Nguyen-Yamamoto², Reyhaneh Salehi-Tabar¹, Michela Zago⁵, Jorg H. Fritz^{1,3,4}, Carolyn J. Baglolo^{2,5}, David Goltzman^{1,2} & John H. White^{1,2}

Links between solar UV exposure and immunity date back to the ancient Greeks with the development of heliotherapy. Skin contains several UV-sensitive chromophores and exposure to sunlight can produce molecules, such as vitamin D₃, that act in an endocrine manner. We investigated the role of the aryl hydrocarbon receptor (AHR), an environmental sensor and ligand-regulated transcription factor activated by numerous planar compounds of endogenous, dietary or environmental origin. 15- to 30-minute exposure of cells to a minimal erythemal dose of UVB irradiation *in vitro* induced translocation of the AHR to the nucleus, rapidly inducing site-specific DNA binding and target gene regulation. Importantly, *ex vivo* studies with Ahr wild-type or null fibroblasts showed that serum from mice whose skin was exposed to a 15 min UVB dose, but not control serum, contained agonist activity within 30 min of UV irradiation, inducing AHR-dependent gene expression. Moreover, a 15-min cutaneous UVB exposure induced AHR site-specific DNA binding and target gene regulation *in vivo* within 3–6 hr post-irradiation in blood and in peripheral tissues, including intestine. These results show that cutaneous exposure of mice to a single minimal erythemal dose of UVB induces rapid AHR signaling in multiple peripheral organs, providing compelling evidence that moderate sun exposure can exert endocrine control of immunity through the AHR.

Links between solar ultraviolet (UV) irradiation and immunity date back millennia; the concept of heliotherapy was developed by the ancient Greeks, and reintroduced in the 19th century with the advent of the sanatorium movement in Europe to treat consumption (tuberculosis)¹. Seminal work in the 1970s showed that UV irradiation suppressed systemic cell-mediated immunity in mice against tumor associated antigens². UV light, which is divided into UVC (100–290 nm), UVB (290–320 nm), and UVA (320–400 nm)³, is filtered by the ozone layer such that all UVC and much of the UVB radiation does not reach the earth's surface. This, depending on latitude and the angle of the sun, leaves a variable portion of UVB and most UVA unfiltered. Skin contains numerous UV-sensitive chromophores, leading to the production of several photoproducts upon exposure that can regulate both the innate and adaptive arms of the immune system³. These include trans-urocanic acid, DNA, lipids and tryptophan^{3,4}. Much attention about the endocrine effects of UV exposure has focused on understanding the role of vitamin D₃, produced cutaneously from UVB-induced photo- and thermal conversion of 7-dehydrocholesterol, and recent work has shown that vitamin D signaling can regulate immunity^{4,5}. However, there is evidence that exposure of skin to UVB at levels that induce minimal or no increase in circulating vitamin D metabolites leads to immune system regulation⁶.

While UV exposure can modulate immunity by altering antigen presentation or cytokine levels⁷, other endocrine factors may also be produced by photochemical reactions in exposed skin. There are also candidate endocrine factors that may activate endocrine signaling via the aryl hydrocarbon receptor (AHR)⁸. The AHR is a ligand-regulated transcription factor highly expressed in barrier organs of the body⁹. While it

¹Departments of Physiology, McGill University, Montreal, Quebec, Canada. ²Departments of Medicine, McGill University, Montreal, Quebec, Canada. ³Departments of Microbiology and Immunology, McGill University, Montreal, Quebec, Canada. ⁴Complex Traits Group, McGill University, Montreal, Quebec, Canada. ⁵Meakins-Christie Laboratories, McGill University, Montreal, Quebec, Canada. Correspondence and requests for materials should be addressed to J.H.W. (email: john.white@mcgill.ca)

Received: 5 August 2018

Accepted: 24 May 2019

Published online: 11 June 2019

was initially characterized for its capacity to bind dioxin (2,3,7,8-tetrachlorodibenzodioxin), a potent and metabolically-resistant environmental toxicant, the AHR functions physiologically in epithelial barriers as a sensor of compounds of endogenous, dietary or environmental origin that include a wide array of largely planar molecules^{9–12}. Although endogenous AHR ligands remain elusive, 6-formylindolo[3,2-b]carbazole (FICZ), a tryptophan photoproduct with very high AHR binding affinity has been proposed to be a physiological agonist for AHR¹³. The AHR is a member of the basic helix-loop-helix-PAS (bHLH-PAS) transcription factor family. It heterodimerizes with its homologue ARNT (AHR nuclear translocator) to bind cognate DNA sequences variously called xenobiotic, dioxin, or AHR response elements (XREs, DREs, or AHREs, respectively). The AHR can also heterodimerize with RELB, an anti-inflammatory and immune-modulatory subunit of the transcription factor NF- κ B¹⁴. One of the most strongly induced AHR target genes encodes CYP1A1, which hydroxylates and metabolically inactivates some several physiological AHR ligands of relevance for the immune system^{15–18}.

AHR signaling can be induced locally in the skin and CYP1A1 increases in extra-cutaneous tissues by UVB exposure^{19,20}. Therefore, in this study, we tested the hypothesis that exposure to a single minimal erythemic dose of ultraviolet B radiation can induce systemic AHR signaling *in vivo*. We show that UVB exposure *in vitro* induces nuclear localization of the AHR within 15 min, leading to its site-specific DNA binding and target gene regulation. A series of *ex vivo* and *in vivo* experiments with mice revealed that cutaneous exposure to a single dose of UVB leads to release of AHR agonists into the circulation, and to induced AHR DNA binding and target gene regulation *in vivo* in peripheral tissues within 3 hr after exposure. Taken together, these studies show that UV exposure of skin rapidly induces endocrine signaling through the AHR.

Results and Discussion

To test for effects of single doses of moderate UV exposure on AHR signaling for *in vitro* and *in vivo* studies below, we used an irradiation protocol that generated 1.2 kJ/m² or 2.5 kJ/m² after 15 or 30 min exposures, which is equivalent to approximately 1–2 minimal erythemal doses in mice²¹. Other work has shown that the level of irradiation used produces no or only moderate increases in circulating levels of vitamin D metabolites *in vivo* and thus represents a low physiological dose⁶. We carried out control experiments *in vitro* to test the kinetics of UV-induced nuclear translocation of AHR, using a protocol that generated complete separation of nuclear lamin and cytoplasmic actin (Fig. S1A). Unless otherwise noted, we used a narrow-band (311 nm) UV source for *in vitro* studies because broadband UVB induces elevated levels of cell death *in vitro* even after limited exposure^{22,23}. Under these conditions, a single 10–30 min exposure induced AHR nuclear translocation in well differentiated SCC25 squamous carcinoma and THP-1 cells (Fig. 1A,B) to a degree that was similar to that induced by AHR agonist FICZ (Fig. 1C). A similar degree of AHR nuclear translocation was also observed in HaCaT keratinocytes following a single 15 min exposure to UVB (Fig. S1B). In other control experiments, a single dose of UV had no effect on the subcellular localization of the vitamin D receptor after 1 hr, although addition of the AHR activator kynurenine led to accumulation of the AHR in the nucleus over the same period (Fig. S1C,D), indicating that there was not a general effect on nucleocytoplasmic shuttling arising from UV exposure. Light-activated AHR signaling has been observed in a variety of cultured cells since the first report by Paine in 1976²⁴, and the functional relevance of tryptophan as an UVB chromophore for formation of an endogenous AHR-activating photoproduct that explains the effect of light on cells has been repeatedly documented^{13,25–28}.

To probe further the effects of UVB exposure on AHR activation, we analyzed expression of the well-characterized AHR target gene, CYP1A1, 4 hr after 15 min UVB exposure, which revealed an induction in SCC25 cells that was approximately 2-fold higher than that induced by FICZ after the same period (Fig. 1D). Induction of CYP1A1 expression was also observed in similar experiments with HaCaT keratinocytes and human THP-1 macrophages (Fig. S2A,B). Note that we observed AHR-specific induction of CYP1A1 expression in SCC25 cells exposed for 5 to 20 min to the same dose of broadband UV (Fig. S2C). Furthermore, a single dose of narrow band UVB led to sustained CYP1A1 expression at least 72 hr after exposure in SCC25 epithelial cells (Fig. S2D).

The effects of treatment on AHR target gene regulation were substantiated further by Western blot analysis of CYP1A1 protein, which revealed an increase in expression over a 24 hr period after 15 min of UVB exposure (Fig. 1E). The role of the AHR in UVB-stimulated gene expression was confirmed by depletion of the receptor in SCC25 cells, which abolished induced expression of CYP1A1 and AHR target gene IL1B. These studies were performed using either a single siRNA targeting AHR (Fig. 1F) or pooled siRNAs recognizing completely independent sites on the transcript (Fig. S2E), with similar results. The efficacy of the single siRNA was confirmed in previous studies²⁹, whereas the pooled siRNAs were validated by western blots with two different anti-AHR antibodies (Fig. S2F). A similar knockdown experiment in SCC25 cells abolished induction of CCL1 and S100A9 (Fig. S2G), previously identified as target genes²⁹. Finally, we used Chromatin immunoprecipitation (ChIP) assays (Fig. 2A–C) to test the effects of UV exposure on AHR DNA binding to previously characterized XREs in the promoters of the CYP1A1, IL10, and IL23A genes, all of which, along with AHR target gene IL22, are inducible by AHR agonists or by UVB (Figs 1D, S3A,B)²⁹. UVB exposure for 15 min enhanced AHR DNA binding to XREs of target promoters in SCC25, HaCaT and THP1 cells (Fig. 2A–C).

Collectively, the *in vitro* experiments above show that moderate UVB exposure induces AHR signaling within minutes. Previous work has shown that cutaneous UV exposure in rodents, fish and humans induces AHR function locally in skin and can induce CYP1A1 or other monooxygenases internally^{28,30–34}. To test for the effects of a single, moderate UVB dose on AHR signaling in mice, we used a broadband UV source (peak at 313 nm), which is more reflective of the composition of sunlight than narrowband UV. Initial controls showed that a single exposure of mice to UVB for 15 min (1.2 kJ/m²) induced expression of AHR target genes *Cyp1a1*, *Il22* and *Il23a* in skin (Fig. S4), consistent with previous studies using a higher dose of UV²⁸. To extend these findings, and test whether AHR ligands are released into the circulation rapidly after exposure of mouse skin to UVB, serum was collected from male or female control or UVB-exposed animals 30 min after 15 min of irradiation, and incubated

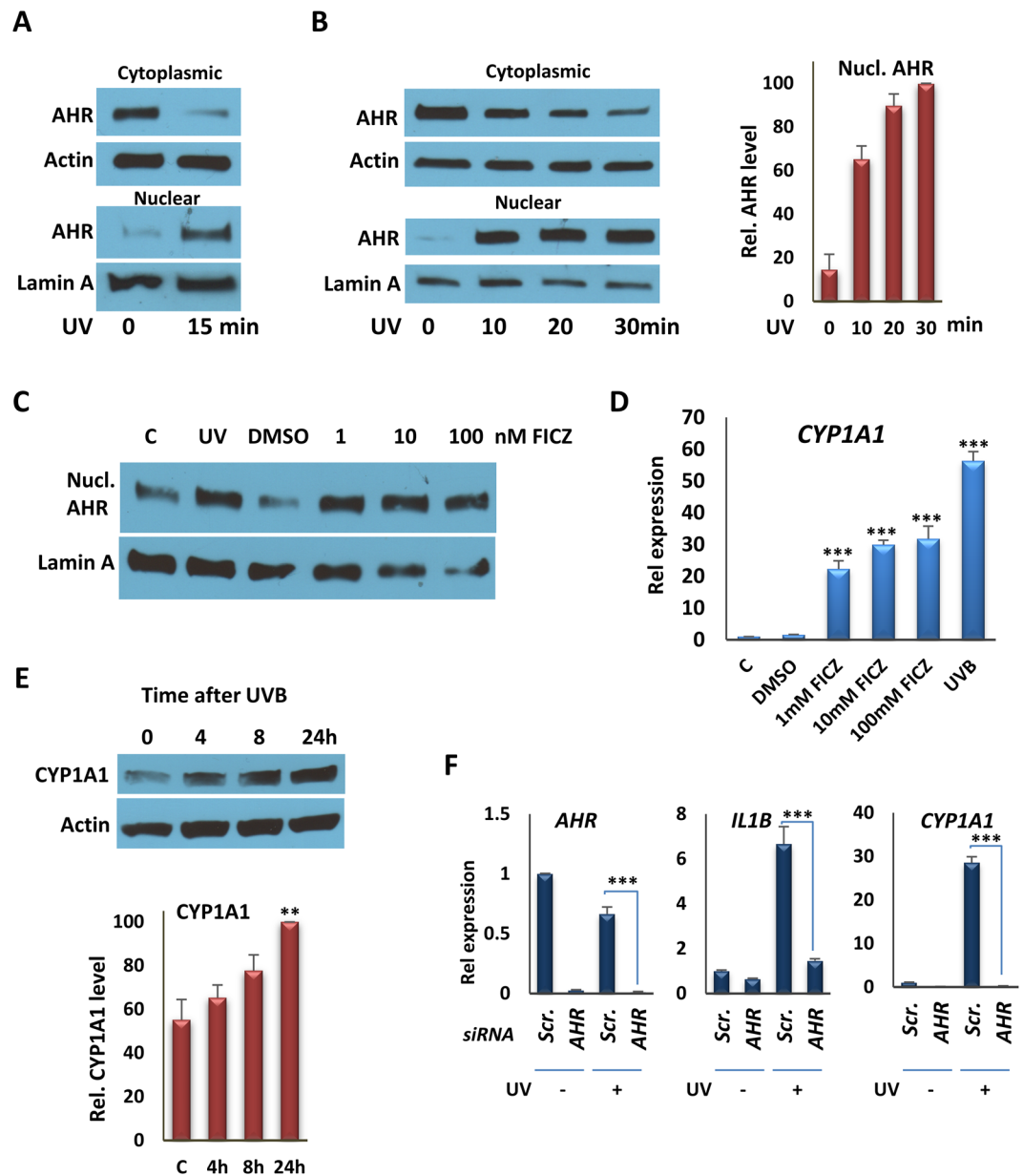


Figure 1. UVB induces AHR translocation to the nucleus and the expression of its target genes, *in vitro*. (A) Western Blot analyses of AHR from nuclear and cytoplasmic fractions from SCC25 cells 1 hr following irradiation with 15 min UVB. Actin was probed as a cytoplasmic marker; lamin A was probed as a nuclear marker. AHR and the internal controls were taken from the same blot. Blot images are provided in the Supplementary Fig. S5A. (B) (left panel) Western Blot analyses of AHR in nuclear and cytoplasmic fractions from THP-1 cells 1 hr following irradiation with UVB (10, 20, or 30 min). (right panel) The quantification of Western Blot analyses, represented in the left panel. AHR and the internal controls were taken from the same blot. Blot images are provided in the Supplementary Fig. S5B. (C) Western Blot analyses of nuclear AHR 1 hr following irradiation with UVB (15 min) or FICZ (1, 10, or 100 nM) treatment. AHR and the internal controls were taken from the same blot. Blot images are provided in the Supplementary Fig. S5C. (D) RT-qPCR analysis of *CYP1A1* transcription in SCC25 cells 4 hr after exposing cells to UVB for 15 min or treating them with FICZ, as indicated. (E) Effect of a single 15 min UVB exposure on production of CYP1A1 protein in SCC25 cells 4, 8 or 24 hr after exposure. (Upper) Western blot of a single experiment. (Lower) Quantification of results of three independent experiments. CYP1A1 and Actin were taken from the same blot. Blot images are provided in the Supplementary Fig. S5D. (F) RT-qPCR analysis of *AHR*, *CYP1A1* and *IL1B* expression in SCC25 cells 4 hr after exposing cells to UVB for 15 min following knockdown of the *AHR* gene with siRNA #1. ** $P < 0.01$, *** $P < 0.001$ as determined by one-way ANOVAs followed by Tukey's post hoc test for multiple comparisons.

with primary fibroblasts derived from wild-type or *Ahr*-null animals. We used primary fibroblasts because standard protocols were available for their culture from wild-type and *Ahr*-null animals and the wild-type cells are highly AHR responsive. Incubation with serum from irradiated but not control mice induced AHR target gene

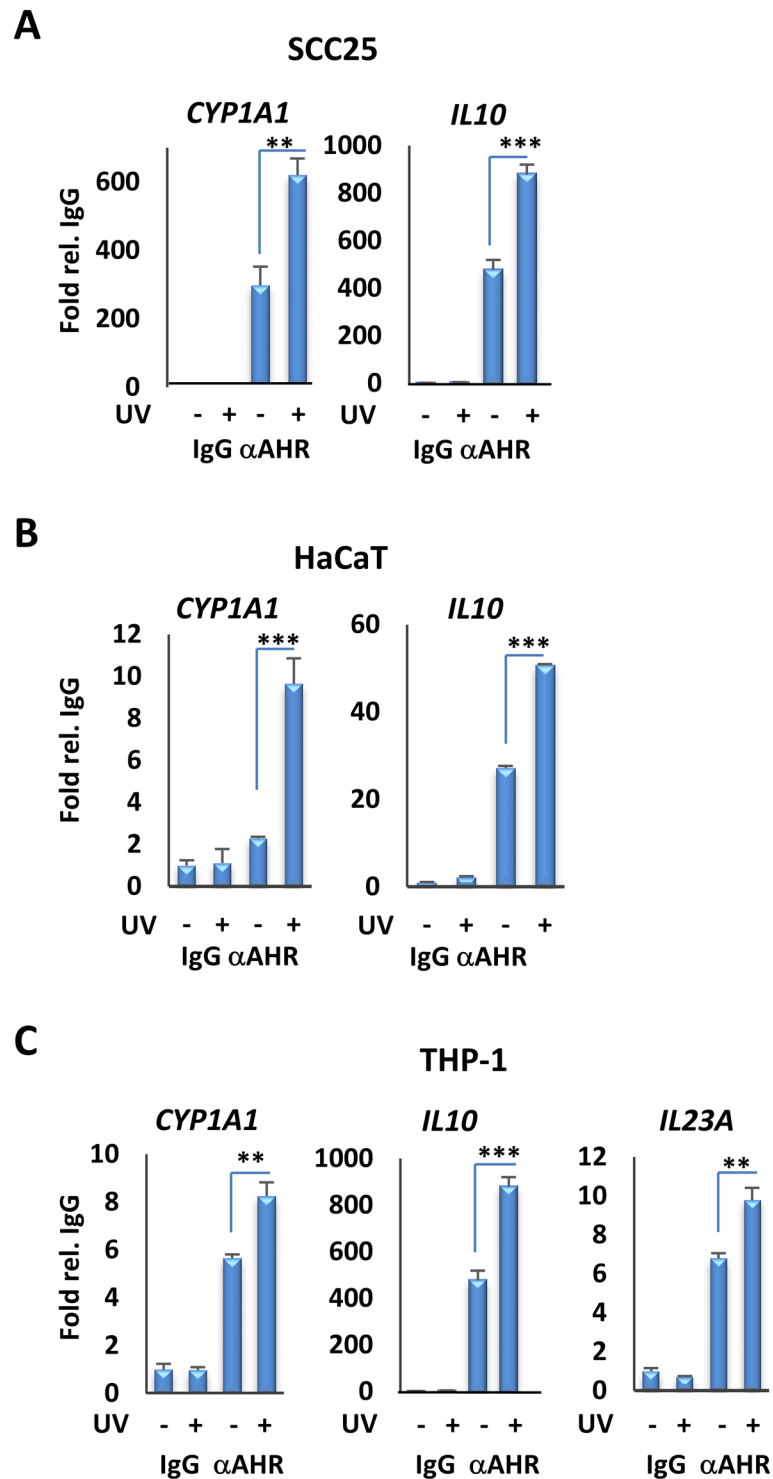


Figure 2. UVB induces AHR recruitment to the promoter of target genes. (A) Analysis of AHR recruitment to the XRE motifs of the *CYP1A1* and *IL10* promoters by ChIP assays, followed by qPCR, in SCC25 cells 4 hr after irradiation with UVB for 15 min. (B) Analysis of AHR recruitment to the XRE motifs of promoters of the *CYP1A1* and *IL10* genes by ChIP assay followed by qPCR, in HaCaT cells 4 hr after irradiation with UVB for 15 min. (C) Analysis of AHR recruitment to the XRE motifs of promoters of the *CYP1A1*, *IL10* and *IL23A* genes by ChIP assays followed by qPCR, in THP-1 cells 4 hr after irradiation with UVB for 15 min. ** $P \leq 0.01$, *** $P \leq 0.001$ as determined by one-way ANOVAs followed by Tukey's post hoc test for multiple comparisons.

expression in wild-type but not *Ahr*-null fibroblasts (Fig. 3A). Furthermore, the effect in wild-type fibroblasts was completely blocked by the AHR antagonist CH223191 (Fig. 3A). These experiments show that moderate UVB exposure of skin leads to rapid (within 30 min) release into the circulation of agonists that induce robust AHR

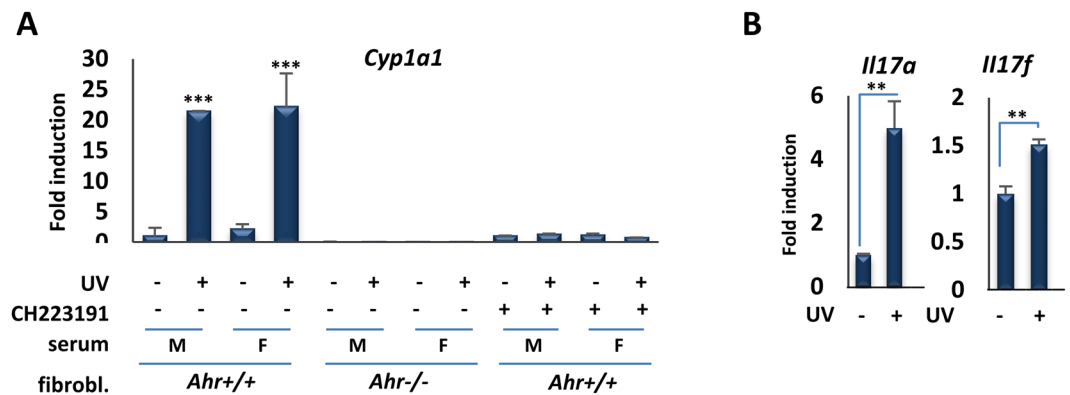


Figure 3. Serum of mice exposed to moderate UVB induces the expression of AHR target genes, *ex vivo*. (A) Serum of UVB-exposed mice induces the expression of AHR target genes in mouse fibroblast. RT-qPCR assay of *Cyp1a1* mRNA expression in primary fibroblasts derived from wild-type or *Ahr*-null mice 6 hr following treatment with the serum of control unexposed (–) mice or UV-exposed (+) male or female mice and AHR inhibitor, CH223191. Serum obtained from mice 30 min after irradiation with (1.2 kJ/m²) UVB for 15 min. (B) *Il17a* and *Il17b* gene expression following incubation of naïve T cells with sera from UVB-exposed mice. ***P* ≤ 0.01, ****P* ≤ 0.001 as determined by one-way ANOVAs followed by Tukey's post hoc test for multiple comparisons.

target gene expression, consistent with the kinetics of AHR induction *in vitro* seen above. This effect is dependent on the presence of the receptor but independent of the sex of mice providing either donor serum or recipient fibroblasts. In addition, incubation of sera from UVB-exposed but not control animals with naïve T cells induced expression of Th17 markers *Il17a* and *Il17b* (Fig. 3B), consistent with the capacity of AHR agonists to induce Th17 cell differentiation¹⁶.

Taken together, studies above reveal serum derived from animals exposed to moderate levels of UVB induces robust AHR signaling *ex vivo*. To test for the effects of UV exposure on induction of AHR signaling in peripheral tissues *in vivo*, we determined the effects of a single 1.2 kJ/m² dose of UVB on the expression of several receptor target genes in blood, liver or intestine, 3 or 6 hr after UVB exposure, as indicated (Fig. 4A–D). Previous studies have shown that the AHR is expressed in T cell and myeloid cell populations in blood^{16,35,36}, in hepatocytes and endothelial cells in liver^{37,38} and in ILC2 innate lymphoid cells in the intestine^{11,39}. In all cases, induction of AHR target genes expression was observed in these peripheral tissues (Fig. 4A–D), consistent with cutaneous UVB exposure inducing rapid, endocrine signaling. Target genes included *Il22* and *Il23a* in intestine were upregulated, consistent with the effects of UVB on their expression *in vitro* (Fig. S3). IL23 is a macrophage cytokine that is a target of AHR signaling in human and mouse²⁹, and part of an AHR-regulated cascade; its signaling leads to production of the innate immune cytokine IL22 in AHR-regulated innate lymphoid cells in the intestine⁴⁰. These results were strongly supported by ChIP analysis of AHR DNA binding to well-characterized XREs *in vivo*. In control experiments, a single UVB dose induced AHR binding to XREs in the *Cyp1a1* and *Il23a* promoters in skin (Fig. 5A). The same exposure also stimulated AHR DNA binding in small intestines 6 hr after UVB exposure (Fig. 5B).

Our results along with literature data presented above provide compelling evidence that a single exposure to as little as 15 min of moderate intensity UVB irradiation leads to rapid activation, nuclear translocation, DNA binding, and target gene regulation by the AHR *in vitro* and *in vivo*. Our *in vivo* findings extend observations that cutaneous UV exposure induces local signaling in skin as well as in extra-cutaneous tissues^{28,30,31,34}. UV exposure generated sufficient levels of AHR agonist *in vitro* to induce nuclear translocation within 15 min. Similarly, *ex vivo* studies with serum from UV-exposed mice harvested 30 min after single-dose exposure showed the AHR agonist activity is released rapidly into the circulation following UV treatment. Notably, several indole-containing compounds can serve as AHR ligands^{8,12}. For example, the indole-containing amino acid tryptophan can produce AHR ligands via several routes, including photodimerization to produce FICZ, and condensation with cysteine to produce ITE [2-(1^H-indole-3'-carbonyl)-thiazole-4-carboxylic acid methyl ester]^{41,42}. In this regard, it is noteworthy that FICZ metabolites can be found in the urine of humans⁴³. In experiments conducted with peripheral tissues of UV-exposed mice, we observed induced AHR DNA binding and target gene activation within 3–6 hr in tissues including small intestine, an important site of AHR signaling^{9,11}. Regulatory events in small intestine included AHR binding to and induction of the direct target gene encoding *Il22*, an innate immune cytokine and a key component of AHR-regulated intestinal immunity, as well as induction of the gene encoding *Il23a*, whose signaling lies upstream of *Il22*. Taken together, these data provide compelling evidence that moderate cutaneous UVB exposure induces endocrine signaling through the AHR, a ligand-regulated environmental sensor. These findings are also supported by our observations and those of others that UV exposure induces hepatic P450 activities given the emerging role of AHR signaling in the immune system in mice as well as humans, in particular in barrier organs, our data provide further mechanistic evidence for a role of cutaneous UVB exposure in the endocrine regulation of immunity.

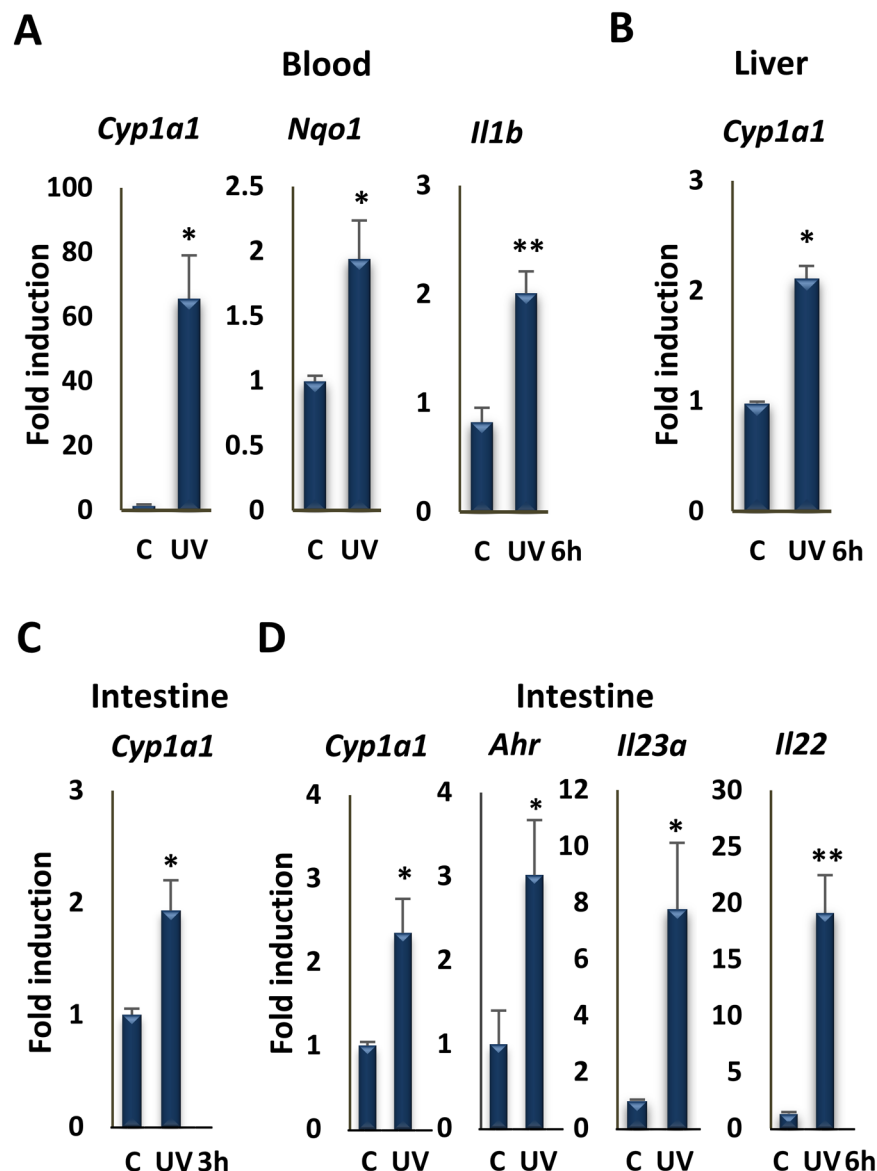


Figure 4. UVB irradiation induces the expression of AHR target genes in different tissues. (A) RT-qPCR assay of *Cyp1a1*, *Nqo1*, and *Il1b* mRNA expression in blood of mice 6 hr following irradiation with 1.2 kJ/m² UVB for 15 min (n = 3 per group). (B) RT-qPCR assay of the *Cyp1a1* mRNA expression in liver of mice 6 hr following irradiation with UVB for 15 min (n = 3 per group). (C) RT-qPCR assay of the *Cyp1a1* mRNA expression in intestine of mice 3 hr following irradiation with UV for 15 min (n = 3 per group). (D) RT-qPCR assay of the *Cyp1a1*, *Ahr*, *Il23a* and *Il22* mRNA expression in intestine of mice 6 hr following irradiation with UVB for 15 min (n = 3 per group). *P ≤ 0.05, **P ≤ 0.01, as determined by one-way ANOVAs followed by Tukey's post hoc test for multiple comparisons.

Materials and Methods

Tissue culture. SCC-25 cells (CRL1628; ATCC) were cultured in DMEM/F12 (319-085-CL; Wisent) supplemented with 10% FBS (non-heat inactivated). HaCaT cells (a gift from the laboratory of Dr. Jean-Jacques Lebrun, McGill University), which are immortalized keratinocytes, were cultured in DMEM (319-005-CL, Wisent Bioproducts) supplemented with 10% FBS. THP-1 monocytic cells (TIB-202; ATCC) were cultured as suspension cells in RPMI 1640 (350-005-CL, Wisent) with 10% FBS (non-heat inactivated; Wisent) and differentiated into adherent THP-1 macrophages with phorbol myristate acetate (PMA; 100 ng/ml) for 24 hr. The *Ahr* knock-out mouse fibroblasts were cultured in EMEM (30-2003; ATCC) supplemented with 15% FBS. Cells were tested for mycoplasma regularly using a Venor™ GeM Mycoplasma Detection Kit (Sigma).

Isolation and culture of mouse primary lung fibroblasts. For isolation of primary lung fibroblast cells from C57BL/6 wild-type mice, a previous published protocol was used⁴⁴. Briefly, after sacrificing the mice, lungs were immediately transferred to the ice-cold PBS. Lung tissue was cut into ~1 mm pieces, washed with

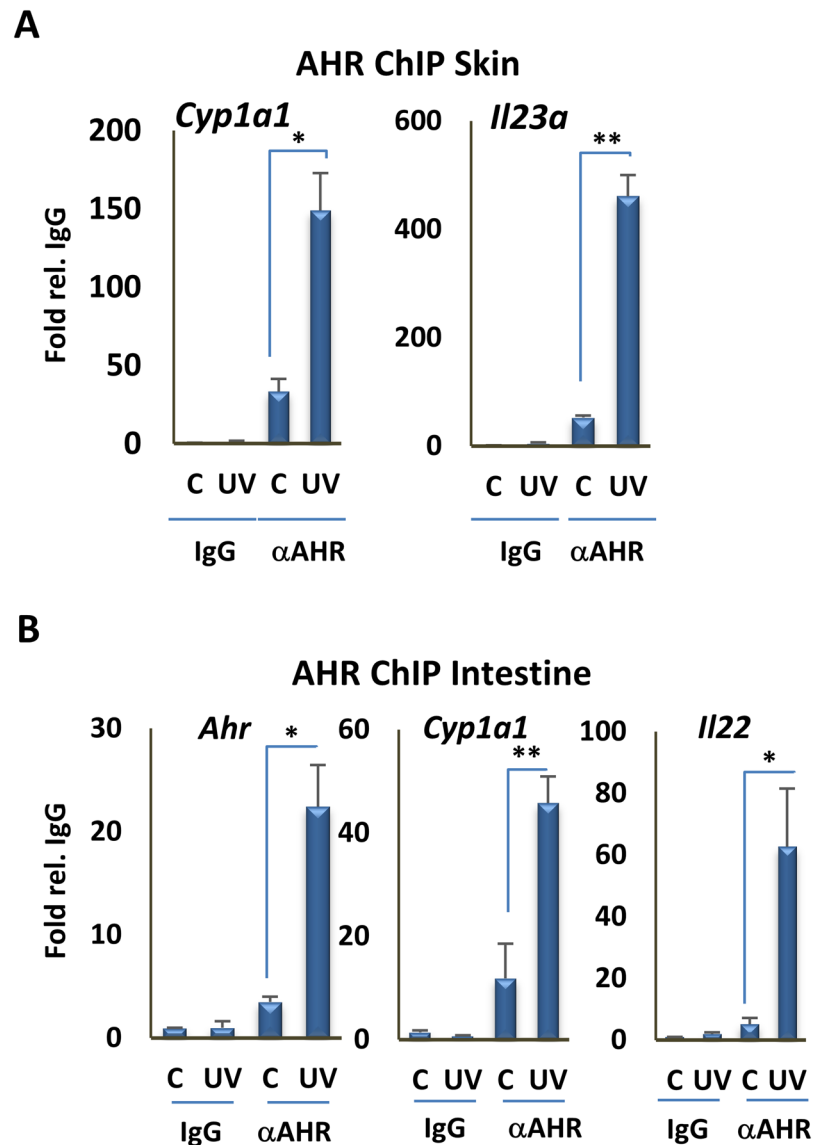


Figure 5. UVB irradiation induces the recruitment of AHR to the promoter of its target genes in different tissues. **(A)** Analysis of AHR recruitment to XRE motifs of the *Cyp1a1* and *Il23a* promoters by ChIP assay, followed by qPCR, in skin of control and UVB-exposed mice (n = 3 per group). **(B)** Analysis of AHR recruitment to the XRE motifs of the *Cyp1a1*, *Ahr*, and *Il22* promoters by ChIP assays followed by qPCR, in intestine of mice 6 hr following irradiation with UVB for 15 min (n = 3 per group). *P ≤ 0.05, **P ≤ 0.01, ***P ≤ 0.001 as determined by one-way ANOVAs followed by Tukey's post hoc test for multiple comparisons.

ice-cold PBS and placed in DMEM/F12 medium containing 0.14 Wunsch units/mL “Liberase TM” and Pen-Strep and kept with gentle shaking at 37°C in cell incubator for 30 min. Cells and tissue fragments were washed with DMEM/F12 + 15% FBS, three times to inactivate liberase and cultured in DMEM/F12 (319-085-CL; Wisent) + 15% FBS + Pen-Strep for up to 14 days. After attaching of the cells to the plate, medium was changed to EMEM (30-2003; ATCC) supplemented with 15% FBS.

Western blot assay and antibodies. Cells were lysed by adding 300 μ l of lysis buffer (0.5% IGEPAL-CA-630 Sigma, 0.5 mM EDTA, 20 mM Tris-Base pH 7.6, 100 mM NaCl, protease inhibitor cocktail) into 10 cm plates. All plates were scraped and transferred into 1.5 ml vial on ice and sonicated in an ice bath for two cycles 10 sec, amplitude 30% on the Vibra-Cell Sonics system VCX-750 (Four-element probe, 3 mm stepped microtip). All vials were centrifuged at 10,000 RPM for 10 min at 4°C. The protein concentration was determined using Bio-Rad DC Protein assay. The normalized and denatured protein samples (containing Laemmli buffer, heated at 70°C 10 min) were loaded on Precast Bio-Rad Mini-TGX 4–15% polyacrylamide gel (456–1084). The following antibodies were used for immunoblotting: AHR (BML-SA210-0100; ENZO Lifesciences), AHR (sc-5579; Santa Cruz), Actin (sc-1615; Santa Cruz), CYP1A1 (sc-393979; Santa Cruz), and VDR (sc-13133; Santa Cruz). Full-sized blots for all westerns shown in the figures are presented in Figs S5 and S6.

Nuclear and cytoplasmic protein extraction. Cells were lysed in lysis buffer (0.5% Nonidet P-40, 0.5 mM EDTA, 20 mM Tris [pH 7.6], 100 mM NaCl, Sigma protease inhibitor cocktail), followed by centrifugation at 700 rcf (g). The supernatant was collected as the cytoplasmic protein fraction. The cytoplasmic fraction in this protocol contains all cell components except nucleus. The pellet (nuclei) was dissolved in RIPA buffer (150 mM NaCl, 1.0% IGEPAL, 0.5% sodium deoxycholate, 0.1% SDS, and 50 mM Tris, pH 8.0) and sonicated at 35% power for 3 cycles of 10 sec, then centrifuged at 10000 RPM. The supernatant used as the nuclear fraction.

Small interfering RNA-mediated knockdown. The following siRNAs were used for knockdown: negative control siRNA (non-silencing; SI03650325; QIAGEN); siRNA #1: Hs_AHR_6 FlexiTube siRNA (SI03043971; QIAGEN). ON-TARGETplus non-targeting siRNAs (D-001810-0X; Dharmacon); siRNA #2: SMART pool ON-TARGETplus human AHR siRNA (L-004990-00-0005; Dharmacon). siRNA knockdowns were performed as described previously²⁹.

RNA extraction. For cell culture, RNA extraction was initially performed by using 1 ml TRIzol reagent or Tri-Reagent (Favorgen). Cells were homogenized by pipetting up and down several times and transferred into 1.5 ml vial. 200 μ l chloroform was added, and the vials were shaken horizontally for 15 sec and kept for 10 min at room temperature and then centrifuged at 10,000 RPM for 10 min at 4 °C. Next, 400 μ l of supernatant was passed through the first column (white) of a Blood/Cultured Cell Total RNA Mini Kit (FABRK Favorgen), and mixed with the same volume of 70% ethanol, and passed through the RNA extraction second column (red). The RNA was washed and eluted according to the manufacturer's Favorgen instructions. Tissues were frozen using dry ice or the flash frozen method immediately after sacrificing the mice. RNA was isolated from tissues by pulverizing with a Scienceware liquid nitrogen cooled mini mortar and pestle set, and about the size of a match head dissolved by pipetting in 1 ml TRIzol reagent or Tri-reagent (Favorgen). 200 μ l chloroform was added, shaken horizontally for 15 sec, and kept at room temperature (RT) for 10 min. The remaining steps are similar to those for RNA extraction from cells. For blood, 200 μ l of blood were mixed with in 1 ml TRIzol-LS. Small intestine was used for RNA extraction from intestinal tissue.

Quantitative PCR. cDNA was prepared from 500 ng of total RNA. Reverse transcription (RT) was performed with iScript cDNA Synthesis Kit (170-8891; Bio-Rad), and qPCR was performed using SsoFast EvaGreen Supermix (172-5211; Bio-Rad) on an Illumina Eco qPCR cycler. Primers used for analysis of gene expression are in Table S1.

Chromatin immunoprecipitation (ChIP) assay. ChIP assays were performed as previously described²⁹. AHR Ab (sc-5579; Santa Cruz) and normal rabbit IgG (2729; Cell Signaling) were used for ChIP assays. Primer sequences used in qPCR for ChIP analysis are listed in Table S1.

Mice. 3–4 months-old C57BL/6 in-house bred mice were used. The baseline expression of Cyp1a1, as a marker of AHR activity, was checked in in-house bred mice and ordered mice; we observed lower baseline Cyp1a1 expression in in-house bred mice compare to ordered mice. All animal experiments were reviewed and approved by the McGill University Animal Care Committee and all experiments were performed in accordance with the relevant guidelines and regulations.

UV irradiation. The backs of the mice were shaved and 24 hr later mice were injected with ketamine hydrochloride and irradiated with broadband FS20T12/UVB Bulb (two lamps) from 40 cm distance for 15 or 30 min. For *in vitro* experiments, SCC-25 or THP-1 cells were cultured in 6 or 10 cm plates, and cells were irradiated in plates without lid under a biological hood using UVB narrowband TL20W/01-RS (two lamps) from 40 cm distance for 15 min or the times indicated in the figures. For cell culture experiments, only narrowband UVB lamps were used, because broadband lamps cause significant cell apoptosis and detachment. TL20W/01RS lamps emit a narrow peak around 311 nm, whereas FS20T12/UVB lamps emit a continuous spectrum from 275 to 390 nm, with a peak emission at 313 nm. Approximately, 65% of that radiation is within the UVB wavelength range.

Mouse serum preparation. Following UV irradiation, mice were sacrificed and approximately 1 ml blood was obtained by cardiac puncture. The blood was kept vertically in vial for 30 min at room temperature in the dark to allow the blood to clot in an upright position and no movement, and then centrifuged for 10 min at 3000 RPM. The serum was transferred to new vial. Centrifugation was repeated, for 5 min, in case of presence of blood or transparent viscous material in the supernatant (serum).

Naïve T cell isolation from spleen. Naïve T cells were isolated by EasySepMouse Naïve CD4⁺ T Cell Isolation Kit (19765; Stemcell) from mouse spleen. Mice were anesthetized by ketamine and spleens were transferred in cold Hanks' Balanced Salt Solution containing 2% fetal bovine serum (FBS) and disrupted. All aggregates and debris were removed by passing the suspension through a 70 μ m nylon strainer and centrifuged at 300 \times g for 10 min and re-suspended at 1×10^8 nucleated cells/mL in recommended medium. Antibody-based cell depletion was performed as per manufacturer's recommendations.

Th17 polarization of mouse CD4 cells. Naïve T cells need activation for proliferation. For activation of naïve T cells, the protocol from BioLegend Inc. was used, as previously published⁴⁵. Bacterial plastic petri dishes (higher affinity for coating) were coated with anti-mouse CD3 ϵ (clone 145-2C11, 2 μ g/ml) and incubated at 37 °C for 2 hr or 4 °C overnight. All dishes were washed 3 times with sterile PBS. Then CD4 cells were added at 1×10^6 /ml to the plates and cultured for 3 days in the presence of anti-mouse CD28 (clone 37.51, 5 μ g/mL), IL-6 (50 ng/mL), TGF- β 1 (1 ng/mL), anti-mouse IL-4 (10 μ g/mL), anti-mouse IFN- γ (10 μ g/mL). Then

non- and UVB-exposed-mouse serum were added into two separate plates. At day 3, cells were washed once and re-stimulated in complete medium with 500 ng/ml PdBu + 500 ng/mL ionomycin, in the presence of Brefeldin A for 4 hr. List of antibodies and cytokines is as follows: Anti-mouse CD3 ϵ (clone 145-2C11, LEAF format, cat. # 100314), Anti-mouse CD28 (clone 37.51, LEAF format, cat. # 102112), Anti-mouse IL-4 (LEAF format, cat # 504108), Anti-mouse IFN- γ (LEAF format, cat. # 505812), Recombinant mouse IL-6 (carrier-free, cat. # 575702), Recombinant human TGF- β 1 (carrier-free, cat. # 580702), Recombinant mouse IL-23 (carrier-free, cat. # 589002), Brefeldin A (cat. # 420601), PdBu (Phorbol 12, 13-dibutyrate; cat. # P1269; Sigma) were used for Th17 Polarization.

Statistical analysis. All experiments are representative of three to five biological replicates. Statistical analysis was conducted using SYSTAT13 Trial by performing one-way ANOVA, followed by the Tukey test for multiple comparisons.

References

- Masten, A. R. Sunlight in Tuberculosis. *Chest* **1**, 8–23, <https://doi.org/10.1378/chest.1.7.8> (1935).
- Fisher, M. S. & Kripke, M. L. Systemic alteration induced in mice by ultraviolet light irradiation and its relationship to ultraviolet carcinogenesis. *Proceedings of the National Academy of Sciences* **74**, 1688, <https://doi.org/10.1073/pnas.74.4.1688> (1977).
- Leitenberger, J., Jacobs, H. T. & Cruz, P. D. Jr. Photoimmunology - illuminating the immune system through photobiology. *Seminars in Immunopathology* **29**, 65–70, <https://doi.org/10.1007/s00281-007-0063-6> (2007).
- Hart, P. H., Gorman, S. & Finlay-Jones, J. J. Modulation of the immune system by UV radiation: more than just the effects of vitamin D? *Nat Rev Immunol* **11**, 584–596 (2011).
- White, J. H. Vitamin D metabolism and signaling in the immune system. *Reviews in Endocrine & Metabolic Disorders* **13**, 21–29, <https://doi.org/10.1007/s11154-011-9195-z> (2012).
- Becklund, B. R., Severson, K. S., Vang, S. V. & DeLuca, H. F. UV radiation suppresses experimental autoimmune encephalomyelitis independent of vitamin D production. *Proceedings of the National Academy of Sciences of the United States of America* **107**, 6418–6423, <https://doi.org/10.1073/pnas.1001119107> (2010).
- Norval, M., McLoone, P., Lesiak, A. & Narbutt, J. The effect of chronic ultraviolet radiation on the human immune system. *Photochem. Photobiol.* **84**, 19–28, <https://doi.org/10.1111/j.1751-1097.2007.00239.x> (2008).
- Quintana, F. J. & Sherr, D. H. Aryl hydrocarbon receptor control of adaptive immunity. *Pharmacological reviews* **65**, 1148–1161, <https://doi.org/10.1124/pr.113.007823> (2013).
- Li, Y. *et al.* Exogenous stimuli maintain intraepithelial lymphocytes via aryl hydrocarbon receptor activation. *Cell* **147**, 629–640, <https://doi.org/10.1016/j.cell.2011.09.025> (2011).
- Esser, C. & Rannug, A. The aryl hydrocarbon receptor in barrier organ physiology, immunology, and toxicology. *Pharmacological reviews* **67**, 259–279, <https://doi.org/10.1124/pr.114.009001> (2015).
- Kiss, E. A. *et al.* Natural Aryl Hydrocarbon Receptor Ligands Control Organogenesis of Intestinal Lymphoid Follicles. *Science* **334**, 1561–1565, <https://doi.org/10.1126/science.1214914> (2011).
- Esser, C., Rannug, A. & Stockinger, B. The aryl hydrocarbon receptor in immunity. *Trends in Immunology* **30**, 447–454 (2009).
- Rannug, A. *et al.* Certain photooxidized derivatives of tryptophan bind with very high affinity to the Ah receptor and are likely to be endogenous signal substances. *J Biol Chem* **262**, 15422–15427 (1987).
- Quintana, F. J. The aryl hydrocarbon receptor: a molecular pathway for the environmental control of the immune response. *Immunology* **138**, 183–189, <https://doi.org/10.1111/imm.12046> (2013).
- Nebert, D. W., Dalton, T. P., Okey, A. B. & Gonzalez, F. J. Role of aryl hydrocarbon receptor-mediated induction of the CYP1 enzymes in environmental toxicity and cancer. *Journal of Biological Chemistry* **279**, 23847–23850, <https://doi.org/10.1074/jbc.R400004200> (2004).
- Veldhoen, M. *et al.* The aryl hydrocarbon receptor links T(H)17-cell-mediated autoimmunity to environmental toxins. *Nature* **453**, 106–111, <https://doi.org/10.1038/nature06881> (2008).
- Schiering, C. *et al.* Feedback control of AHR signalling regulates intestinal immunity. *Nature* **542**, 242–245, <https://doi.org/10.1038/nature21080> (2017).
- Effner, R. *et al.* Cytochrome P450s in human immune cells regulate IL-22 and c-Kit via an AHR feedback loop. *Scientific Reports* **7**, 44005, <https://doi.org/10.1038/srep44005> (2017).
- Rannug, A. & Fritsche, E. The aryl hydrocarbon receptor and light. *Biological chemistry* **387**, 1149–1157, <https://doi.org/10.1515/bc.2006.143> (2006).
- Ma, Q. Influence of light on aryl hydrocarbon receptor signaling and consequences in drug metabolism, physiology and disease. *Expert opinion on drug metabolism & toxicology* **7**, 1267–1293, <https://doi.org/10.1517/17425255.2011.614947> (2011).
- McGlade, J. P. *et al.* Effect of both ultraviolet B irradiation and histamine receptor function on allergic responses to an inhaled antigen. *Journal of Immunology* **178**, 2794–2802 (2007).
- Cho, T. H., Lee, J. W. & Lee, M. H. Evaluating the cytotoxic doses of narrowband and broadband UVB in human keratinocytes, melanocytes, and fibroblasts. *Photodermatology, Photoimmunology & Photomedicine* **24**, 110–114, <https://doi.org/10.1111/j.1600-0781.2008.00347.x> (2008).
- Tuchinda, C., Lim, H. W., Strickland, F. M., Guzmán, E. A. & Wong, H. K. Comparison of broadband UVB, narrowband UVB, broadband UVA and UVA1 on activation of apoptotic pathways in human peripheral blood mononuclear cells. *Photodermatology, Photoimmunology & Photomedicine* **23**, 2–9, <https://doi.org/10.1111/j.1600-0781.2007.00260.x> (2007).
- Paine, A. J. Induction of benzo[a]pyrene Mono-oxygenase in liver cell culture by the photochemical generation of active oxygen species. Evidence for the involvement of singlet oxygen and the formation of a stable inducing intermediate. *The Biochemical journal* **158**, 109–117 (1976).
- Lorenzen, A., James, C. A. & Kennedy, S. W. Effects of UV irradiation of cell culture medium on PCB-mediated porphyrin accumulation and EROD induction in chick embryo hepatocytes. *Toxicology in Vitro* **7**, 159–166 (1993).
- Wei, Y. D., Rannug, U. & Rannug, A. UV-induced CYP1A1 gene expression in human cells is mediated by tryptophan. *Chem Biol Interact* **118**, 127–140 (1999).
- Oberg, M., Bergander, L., Hakansson, H., Rannug, U. & Rannug, A. Identification of the tryptophan photoproduct 6-formylindolo[3,2-b]carbazole, in cell culture medium, as a factor that controls the background aryl hydrocarbon receptor activity. *Toxicological sciences: an official journal of the Society of Toxicology* **85**, 935–943, <https://doi.org/10.1093/toxsci/kfi154> (2005).
- Fritsche, E. *et al.* Lightning up the UV response by identification of the arylhydrocarbon receptor as a cytoplasmic target for ultraviolet B radiation. *Proceedings of the National Academy of Sciences of the United States of America* **104**, 8851–8856, <https://doi.org/10.1073/pnas.0701764104> (2007).
- Memari, B. *et al.* Engagement of the Aryl Hydrocarbon Receptor in Mycobacterium tuberculosis-Infected Macrophages Has Pleiotropic Effects on Innate Immune Signaling. *The Journal of Immunology* **195**, 4479–4491, <https://doi.org/10.4049/jimmunol.1501141> (2015).

30. Mukhtar, H. *et al.* Additive effects of ultraviolet B and crude coal tar on cutaneous carcinogen metabolism: possible relevance to the tumorigenicity of the Goeckerman regimen. *J Invest Dermatol* **87**, 348–353 (1986).
31. Goerz, G., Merk, H., Bolsen, K., Tsambaos, D. & Berger, H. Influence of chronic UV-light exposure on hepatic and cutaneous monooxygenases. *Experientia* **39**, 385–386, <https://doi.org/10.1007/BF01963137> (1983).
32. Goerz, G. *et al.* Influence of UVA and UVB irradiation on hepatic and cutaneous P450 isoenzymes. *Archives of Dermatological Research* **289**, 46–51, <https://doi.org/10.1007/s004030050151> (1996).
33. Behrendt, L., Jonsson, M. E., Goldstone, J. V. & Stegeman, J. J. Induction of cytochrome P450 1 genes and stress response genes in developing zebrafish exposed to ultraviolet radiation. *Aquatic toxicology (Amsterdam, Netherlands)* **98**, 74–82, <https://doi.org/10.1016/j.aquatox.2010.01.008> (2010).
34. Katiyar, S. K., Mukhtar, H. & Matsui, M. S. Ultraviolet-B Exposure of Human Skin Induces Cytochromes P450 1A1 and 1B1. *J. Invest. Dermatol.* **114**, 328–333 (2000).
35. Frericks, M., Meissner, M. & Esser, C. Microarray analysis of the AHR system: Tissue-specific flexibility in signal and target genes. *Toxicology and Applied Pharmacology* **220**, 320–332, <https://doi.org/10.1016/j.taap.2007.01.014> (2007).
36. Trifari, S., Kaplan, C. D., Tran, E. H., Crellin, N. K. & Spits, H. Identification of a human helper T cell population that has abundant production of interleukin 22 and is distinct from T-H-17, T(H)1 and T(H)2 cells. *Nat. Immunol.* **10**, 864–U873, <https://doi.org/10.1038/ni.1770> (2009).
37. Park, K. T., Mitchell, K. A., Huang, G. M. & Elferink, C. J. The aryl hydrocarbon receptor predisposes hepatocytes to Fas-mediated apoptosis. *Molecular Pharmacology* **67**, 612–622, <https://doi.org/10.1124/mol.104.005223> (2005).
38. Walisser, J. A., Glover, E., Pande, K., Liss, A. L. & Bradfield, C. A. Aryl hydrocarbon receptor-dependent liver development and hepatotoxicity are mediated by different cell types. *Proceedings of the National Academy of Sciences of the United States of America* **102**, 17858–17863, <https://doi.org/10.1073/pnas.0504757102> (2005).
39. Lee, J. S. *et al.* AHR drives the development of gut ILC22 cells and postnatal lymphoid tissues via pathways dependent on and independent of Notch. *Nat. Immunol.* **13**, 144–U158, <https://doi.org/10.1038/ni.2187> (2012).
40. Qiu, J. *et al.* The Aryl Hydrocarbon Receptor Regulates Gut Immunity through Modulation of Innate Lymphoid Cells. *Immunity* **36**, 92–104, <https://doi.org/10.1016/j.immuni.2011.11.011> (2012).
41. Song, J. *et al.* A ligand for the aryl hydrocarbon receptor isolated from lung. *Proceedings of the National Academy of Sciences* **99**, 14694–14699, <https://doi.org/10.1073/pnas.232562899> (2002).
42. Rannug, A. & Rannug, U. The tryptophan derivative 6-formylindolo[3,2-b]carbazole, FICZ, a dynamic mediator of endogenous aryl hydrocarbon receptor signaling, balances cell growth and differentiation. *Critical reviews in toxicology* **48**, 555–574, <https://doi.org/10.1080/10408444.2018.1493086> (2018).
43. Wincent, E. *et al.* The Suggested Physiologic Aryl Hydrocarbon Receptor Activator and Cytochrome P4501 Substrate 6-Formylindolo[3,2-b]carbazole Is Present in Humans. *Journal of Biological Chemistry* **284**, 2690–2696, <https://doi.org/10.1074/jbc.M808321200> (2009).
44. Au - Seluanov, A., Au - Vaidya, A. & Au - Gorbunova, V. Establishing Primary Adult Fibroblast Cultures From Rodents. *JoVE*, e2033, <https://doi.org/10.3791/2033> (2010).
45. Veldhoen, M., Hirota, K., Christensen, J., O'Garra, A. & Stockinger, B. Natural agonists for aryl hydrocarbon receptor in culture medium are essential for optimal differentiation of Th17 T cells. *The Journal of Experimental Medicine* **206**, 43–49, <https://doi.org/10.1084/jem.20081438> (2009).

Acknowledgements

This work was supported by an operating grant from the Canadian Institutes of Health Research (CIHR, PJT-74294) to J.H.W., C.J.B. and J.H.F.

Author Contributions

B.M. conceived the project and performed the experiments. L.N.-Y. and B.M. did the animal work. B.M., M.Z. and R.S.-T. prepared the cells for experiments. J.H.W., J.H.F., C.J.B., D.G. and B.M. designed research and revised the manuscript. J.H.W., B.M. and R.S.-T. analyzed data. B.M. and J.H.W. wrote the paper.

Additional Information

Supplementary information accompanies this paper at <https://doi.org/10.1038/s41598-019-44862-4>.

Competing Interests: The authors declare no competing interests.

Publisher's note: Springer Nature remains neutral with regard to jurisdictional claims in published maps and institutional affiliations.



Open Access This article is licensed under a Creative Commons Attribution 4.0 International License, which permits use, sharing, adaptation, distribution and reproduction in any medium or format, as long as you give appropriate credit to the original author(s) and the source, provide a link to the Creative Commons license, and indicate if changes were made. The images or other third party material in this article are included in the article's Creative Commons license, unless indicated otherwise in a credit line to the material. If material is not included in the article's Creative Commons license and your intended use is not permitted by statutory regulation or exceeds the permitted use, you will need to obtain permission directly from the copyright holder. To view a copy of this license, visit <http://creativecommons.org/licenses/by/4.0/>.

© The Author(s) 2019